Published Ahead of Print on March 8, 2016 as 10.5966/sctm.2015-0155.

STEM CELLS TRANSLATIONAL MEDICINE®

TISSUE-SPECIFIC PROGENITOR AND STEM CELLS

Impaired Angiogenic Potential of Human Placental Mesenchymal Stromal Cells in Intrauterine Growth Restriction

CHIARA MANDÒ,[a,*] PAOLA RAZINI,[b,*] CHIARA NOVIELLI,[a] GAIA MARIA ANELLI,[a] MARZIA BELICCHI,[b,c] SILVIA ERRATICO,[c] STEFANIA BANFI,[b] MIRELLA MEREGALLI,[b,c] ALESSANDRO TAVELLI,[b] MARCO BACCARIN,[d] ALESSANDRO ROLFO,[e] SILVIA MOTTA,[d] YVAN TORRENTE,[b,c,f,†] IRENE CETIN[a,g,†]

Key Words. Pregnancy • Stem cells • Placenta • Intrauterine growth restriction • Mesenchymal stromal cells

ABSTRACT

Human placental mesenchymal stromal cells (pMSCs) have never been investigated in intrauterine growth restriction (IUGR). We characterized cells isolated from placental membranes and the basal disc of six IUGR and five physiological placentas. Cell viability and proliferation were assessed every 7 days during a 6-week culture. Expression of hematopoietic, stem, endothelial, and mesenchymal markers was evaluated by flow cytometry. We characterized the multipotency of pMSCs and the expression of genes involved in mitochondrial content and function. Cell viability was high in all samples, and proliferation rate was lower in IUGR compared with control cells. All samples presented a starting heterogeneous population, shifting during culture toward homogeneity for mesenchymal markers and occurring earlier in IUGR than in controls. In vitro multipotency of IUGR-derived pMSCs was restricted because their capacity for adipocyte differentiation was increased, whereas their ability to differentiate toward endothelial cell lineage was decreased. Mitochondrial content and function were higher in IUGR pMSCs than controls, possibly indicating a shift from anaerobic to aerobic metabolism, with the loss of the metabolic characteristics that are typical of undifferentiated multipotent cells.

STEM CELLS TRANSLATIONAL MEDICINE *2016;5:1–13*

SIGNIFICANCE

This study demonstrates that the loss of endothelial differentiation potential and the increase of adipogenic ability are likely to play a significant role in the vicious cycle of abnormal placental development in IUGR. This is the first observation of a potential role for pMSCs in intrauterine growth restriction, thus leading to new perspectives for the treatment of IUGR.

INTRODUCTION

Mesenchymal cells are the predominant cellular component in placenta and serve as structural support for trophoblast villi and vascular network [1]. In recent investigations, human placental mesenchymal stromal cells (pMSCs) have been isolated according to the meeting criteria proposed by the Mesenchymal and Tissue Stem Cell Committee [2] and the International Society for Cellular Therapy as cells that adhere to untreated plastic surfaces and express CD105, CD73, and CD90 but not CD34, CD14, CD19, CD11b, CD79α, or HLA-DR and that differentiate into osteogenic, adipogenic, and chondrogenic lineages in vitro [3, 4]. Both fetal (from placental membranes and villi) and maternal (from decidua) pMSCs can be isolated from the human placenta, showing similar phenotypes [5–8]. Indeed, the placental maternal side comprises the chorionic villi on one side and maternal decidua on the other. The peripheral region of the placenta on the maternal side that is in contact with the uterine wall (called the basal plate) comprises the chorionic villi on one side and maternal decidua basalis on the other. The significant issue of the presence of maternal cells in human pMSCs cultures was reviewed recently [9].

Despite progress in the characterization of pMSCs, it remains largely unknown to what degree the pMSCs are involved in placenta disease. Investigation of pMSCs may therefore give important hints for pregnancy pathologies linked to placental insufficiency, namely intrauterine growth restriction (IUGR) and preeclampsia (PE) [10]. IUGR and PE are leading causes of maternal and neonatal morbidity and mortality [11, 12]. A specific placental phenotype has been associated

[a]"L. Sacco" Department of Biomedical and Clinical Sciences, Center for Fetal Research Giorgio Pardi, Università degli Studi di Milano, Milan, Italy; [b]Stem Cell Laboratory, Pathophysiology and Transplantation Department, Fondazione IRCCS Ca' Granda Ospedale Maggiore Policlinico, Centro Dino Ferrari, Università degli Studi di Milano, Milan, Italy; [c]Ystem S.R.L., Milan, Italy; [d]Laboratory of Medical Genetics, Fondazione IRCCS Ca' Granda Ospedale Maggiore Policlinico, Milan, Italy; [e]Department of Surgical Science, University of Turin, Turin, Italy, [f]UNISTEM Interdepartmental Centre for Stem Cell Research, Milan, Italy; [g]Department of Mother and Child, Luigi Sacco Hospital, Milano, Italy

[*]Contributed equally.

[†]Contributed equally.

Correspondence: Irene Cetin, M.D., Ph.D., Department of Mother and Child, "L. Sacco" Department of Biomedical and Clinical Sciences, School of Medicine, Università degli Studi di Milano, Luigi Sacco Hospital, via Giovanni Battista Grassi 74, 20157 Milan, Italy. Telephone: 39 0250319804-05; E-Mail: irene.cetin@unimi.it; or Yvan Torrente, M.D., Ph.D., Department of Pathophysiology and Transplantation, Università degli Studi di Milano, Fondazione IRCCS Ca' Granda Ospedale Maggiore Policlinico, via Francesco Sforza 35, 20122 Milan, Italy. Telephone: 39-0255033874; E-Mail: yvan.torrente@unimi.it.

Received July 15, 2015; accepted for publication December 21, 2015.

1066-5099/2016/$20.00/0

http://dx.doi.org/10.5966/sctm.2015-0155

Published Ahead of Print on March 8, 2016 as 10.5966/sctm.2015-0155.

with IUGR [13], characterized by altered transport of oxygen and nutrients [14–17] and impaired mitochondrial content and function [18, 19]. We recently showed altered mitochondrial content and functionality in cytotrophoblast cells isolated from IUGR placentas [11] suggesting compensatory mitochondrial mechanisms that occur under placental vascular insufficiency. Indeed, IUGR placentas present defective vascular transformation and terminal villous formation, with fewer and thinner villi and vessels, especially in the most severe cases, that are differently distributed along the placental surface, as reviewed by Gourvas et al. [20].

Only a few studies have focused on the role of pMSCs in placental insufficiency, and all of them have addressed preeclampsia [1, 21–25]. Human pMSCs isolated from PE placentas and deciduas display decreased proliferation and, interestingly, show proinflammatory and antiangiogenic characteristics [21, 24, 25] that lead to impairment of trophoblast development and invasive capacity and to defects in placental vasculogenesis. Currently, no data have been reported on pMSCs in IUGR.

Here we hypothesize that pMSC phenotype may be involved in the pathogenesis of IUGR. Thus, we performed a study to isolate human pMSCs residing in physiological and IUGR placentas and to characterize them in vitro, in reference to their immunophenotype, cell viability, expansion rate, differentiation potential, and mitochondrial content, in order to evaluate their potential involvement in IUGR placental phenotype.

Materials and Methods

Study Population

Pregnant women were enrolled in the Unit of Obstetrics and Gynecology of the L. Sacco Hospital in Milan, Italy. The study was approved by the institutional ethics committee, and samples were collected with the informed consent of the patients. Human placentas were obtained at elective cesarean delivery (nonlaboring deliveries) from 11 singleton pregnancies.

We studied six pregnancies complicated by IUGR between 32 and 37 weeks of gestation. Gestational age was calculated from the last menstrual period and was confirmed by routine ultrasonography at 11–12 weeks of gestation. We identified growth-restricted fetuses in utero through repeated longitudinal measurements that demonstrated a reduction in fetal growth velocity [17, 26, 27]. Specifically, IUGR was defined by measurements of abdominal circumferences below the 10th percentile of reference values for fetuses of similar ages together with a shift from the growth curve greater than 40 centiles [28]. As an example, this represents a decrease from the 50th centile (measured at 20 weeks) to below the 10th centile (at the time of IUGR diagnosis). Growth restriction was confirmed at birth if the neonatal weight was below the 10th percentile according to Italian standards for birth weight and gestational age [29].

Healthy controls ($n = 5$) were term ($\geq$37 weeks) physiological pregnancies with normal intrauterine growth and appropriate for gestational age birth weight, according to reference ranges for the Italian population [29]. Exclusion criteria were any placental or fetal disease. Indications for cesarean delivery before labor were breech presentation, previous caesarean deliveries, or maternal request. Exclusion criteria for both groups were maternal drug or alcohol abuse and autoimmune diseases. None of the fetuses had abnormal karyotype, genetic syndromes, viral infection, or major malformations.

Sample Collection, Isolation, and Expansion of Cells Derived From Physiological and IUGR Placentas

Placental tissue was collected immediately after cesarean delivery and rapidly rinsed in phosphate-buffered saline (PBS) containing penicillin (200 U/ml) and streptomycin (200 μg/ml) for cell experiments. Placentas were weighed after discarding of the cord, membranes, and excess blood. Full-thickness pieces, 1.5 cm^3, were sampled in different sites of the placental disc and washed in Hanks' balanced saline solution (Sigma-Aldrich, St. Louis, MO, https://www.sigmaaldrich.com). After mechanical separation of placental membranes (PM) from the placental basal disc (PBD), these tissues were enzymatically digested with collagenase IA (Invitrogen, Life Technologies, ThermoFisher Scientific, Carlsbad, CA, https://www.thermofisher.com) and trypsin 2.5% (Invitrogen, Life Technologies, ThermoFisher Scientific,) and incubated in a fully humidified atmosphere of 5% CO_2, 95% air, at 37°C for 45 minutes.

Digested tissues were then filtered and centrifuged at 2000 rpm for 10 minutes, and cells were grown in expansion medium as previously described [30] with the following minor modifications. PM- and PBD-derived cells were plated in six-well tissue culture plates (VWR, Radnor, PA, https://vwr.com), coated with 0.2% gelatin (Sigma-Aldrich), at a density of 10^4 cells/well. Cells were grown in expansion medium composed of Dulbecco's modified Eagle's medium/F-12 (1:1) (Invitrogen, Life Technologies, ThermoFisher Scientific), 10% fetal bovine serum. and 20 ng/ml epidermal growth factor (Miltenyi Biotec, Bergisch Gladbach, Germany, http://www.miltenyibiotec.com/en). Expansion culture media were prepared fresh weekly. Cells were incubated in a fully humidified atmosphere of 5% CO_2, 95% air, at 37°C for several weeks. Every week, living cells were counted with a Burker chamber using trypan blue (Sigma-Aldrich) exclusion method.

Cells were counted and passaged at a confluence of 70%–80% for up to 6 weeks of culture. At each passage, the population doubling (PD) rate was determined by using the formula doubling time = ln(2)/proliferation index, where the proliferation index is calculated as $N(t)$ = the number of cells at time t/the number of cells at time of previous passages ($t - 7$days). The PD of each passage was calculated and added to the PD of the previous passages to generate the cumulative population doubling rate. All counts were performed in triplicate, and data are shown as mean fold ($\pm$SD in percentages of four experiments).

To assess proliferation and viability, samples were analyzed by MTT (3-[31]-2,5-diphenyltetrazolium bromide) activity assay [31] and expressed as percentage of viable cells on the total cell number. Values are expressed as means $\pm$ of three separate experiments.

Colony-Forming Unit Assays

PM- and PBD-derived pMSC cells (5×10^3) from physiological ($n = 5$) and IUGR ($n = 6$) placentas were used for the colony-forming unit-fibroblast (CFU-F) assay. Cells were plated in expansion medium in duplicate in six-well plates. After 14 days of culture in a humidified incubator at 37°C and 5% CO_2, the colonies were stained with 1% crystal violet solution for 5–10 minutes and washed twice with deionized water. Aggregates of cells with a diameter between 1 and 8 mm were identified as colonies and counted under a light microscope (Leica DM6000R, Leica Microsystems, Renens VD, Switzerland, http://www.leica-microsystems.com/) using the software Image-J (National Institutes of Health, Bethesda, MD, http://imagej.nih.gov). pMSCs were also cultured in methylcellulose as described in the supplemental online data.

Published Ahead of Print on March 8, 2016 as 10.5966/sctm.2015-0155.

FACS Analysis of Cells Isolated From Physiological and IUGR Placentas

At 24 hours, 7 days, and 30 days, 10^5 cells were incubated with 7-amino-actinomycin D (7AAD; used to analyze only live cells [BD Biosciences/Pharmingen, San Jose, CA, https://www.bdbiosciences.com) and with the following antibodies: anti-CD34-allophycocyanin (APC) and anti-CD45-APC-CY7 (hematopoietic stem cell markers); anti-CD31-fluorescein isothiocyanate (FITC) (endothelial cell marker); and anti-CD44-FITC, anti-CD105-phycoerythrin (PE), anti-CD29-FITC, anti-CD73-APC, and anti-CD90-PE-Cy5 (mesenchymal cell markers) (Miltenyi Biotec). Isotype-matched mouse immunoglobulins were used as negative controls. After each incubation, performed at 4°C for 20 minutes, cells were washed in PBS, 1% heat-inactivated FCS, and 0.1% sodium azide. Cytometric analyses were performed with a Cytomics FC 500 flow cytometer and 2.1 CXP software (Beckman Coulter, Brea, CA, https://www.beckmancoulter.com). Each analysis included at least 10,000–20,000 events for each gate. A light-scatter gate was set up to eliminate cell debris from the analysis. The percentage of positive cells was assessed after correction for the percentage reactive to an equivalent isotype control.

Cytogenetic Analysis

PM- and PBD-derived pMSC cells (5×10^3) from physiological ($n = 3$) and IUGR ($n = 2$) placentas were tested by chromosome analysis and real-time polymerase chain reaction (PCR) for Y chromosome (SRY) as described in the supplemental online data.

In Vitro Differentiation of pMSCs Isolated From Physiological and IUGR PM and PBD Tissues

Myogenic Differentiation

After in vitro proliferation, human pMSCs were plated in 24-well tissue culture plates, coated with 10 μg/ml laminin (Sigma-Aldrich), in expansion medium. After 3–5 days (70%–80% confluence), they were switched in low-serum (DMEM, 2% horse serum) fusion-promoting medium for myogenic differentiation. After 14 days of culture, differentiated muscle cells were detected by immunostaining with antibodies against α-smooth muscle actin (α-SMA; 1:50 dilution, mouse anti-human; Sigma-Aldrich) and desmin (1:50 dilution, rabbit polyclonal; Abcam Inc., Cambridge, MA). Nuclei were counterstained with 4′,6-diamidino-2-phenylindole. Images were captured using the Leica TCS SP2 confocal system (Leica Microsystems) at 18–20°C.

Osteogenic, Chondrogenic, and Adipogenic Differentiation

Osteogenic, chondrogenic, and adipogenic potential of pMSCs was verified through the use of specific differentiation kits: hMSC Osteogenic BulletKit, hMSC Chondro BulletKit, and hMSC Adipogenic BulletKit (Lonza, Basel, Switzerland, http://www.lonza.com) (supplemental online data).

Tubulogenesis Assay

Expanded human pMSCs were incubated in an endothelial growth medium containing medium 199 (Gibco-BRL, Life Technologies, ThermoFisher Scientific) supplemented with 50 ng/ml vascular endothelial growth factor (VEGF). Cells were seeded at a density of 30,000 cell/cm^2 on six-well plates coated with Matrigel (Corning, Corning, NY, https://www.corning.com/medium)/199 medium (1:1) and incubated in a humidified atmosphere with 5% CO_2, 95% air, at 37°C. After 24 hours, we observed the formation of capillary-like tube structures by using an inverted microscope (Leica DMIRE2). Manual tube identification was performed using ImageJ software. To depict the beginning and ending points of individual tubes on the processed image, three different operators processed four selected images. As result of this process, a tube topology graph was formed that enables the gathering of valuable statistics, such as total tube length. Tube length was compared in normal and IUGR differentiated pMSCs. Human fibroblast cells were used as a negative control. To confirm tubulogenesis, immunostaining with antibody against von Willebrand factor (vWF; diluted 1:50, Dako, Glostrup, Denmark, http://www.dako.com) was performed on capillary-like tube structures. Images were captured by using an inverted microscope (Leica DM 6000R). Endothelial differentiation was confirmed by real-time PCR analysis of CD31 expression levels. Each experiment was performed in triplicate, and for each sample, the median value between the three experiments was reported.

Angiogenic Potential of pMSCs Isolated From Human Physiological and IUGR Placentas

We investigated the angiogenic potential of pMSCs isolated from physiological and IUGR PM and PBD by using a directed in vivo angiogenesis angioreactor (DIVAA) as described in supplemental online data [32].

Gene Expression Analysis of Mitochondrial Biogenesis Activator and Respiratory Chain Complexes

pMSCs were analyzed for the expression of mitochondria-related genes after approximately 30 days of culture in expansion medium. Total RNA was extracted by TRIzol Reagent (Ambion, Life Technologies, ThermoFisher Scientific). After DNase I treatment (New England Biolabs, Ipswich, MA, https://www.neb.com), aimed at removing potentially contaminating DNA, 1.6 μg of total RNA were reverse-transcribed by using the High Capacity cDNA Reverse Transcription Kit (Applied Biosystems, Life Technologies, ThermoFisher Scientific) with random examers. Gene expression of *UQCRC1*, *COX4I1* (two subunits respectively belonging to the III and IV respiratory chain complexes), and *NRF1* (a mitochondrial biogenesis activator) was analyzed by real-time PCR using the 7500 Fast Real-Time PCR System with TaqMan assays (Applied Biosystems, Life Technologies, ThermoFisher Scientific). Expression levels were determined according to the $E^{-\Delta Ct}$/NF formula (GeNorm method [33]), which considers the assay amplification efficiency (E, calculated from a serial dilution curve) and a normalization factor (NF) relative to *PPIA* and *RPL13A* control genes. All samples were reverse-transcribed in duplicate, and cDNA was run in triplicate.

RESULTS

Clinical Data of the Study Population

Individual clinical data of patients included in this study are presented in supplemental online Table 1. No significant differences emerged between groups for maternal age and prepregnancy BMI. As expected, gestational age, and placental and fetal weights were significantly lower in IUGR than physiological pregnancies.

Published Ahead of Print on March 8, 2016 as 10.5966/sctm.2015-0155.

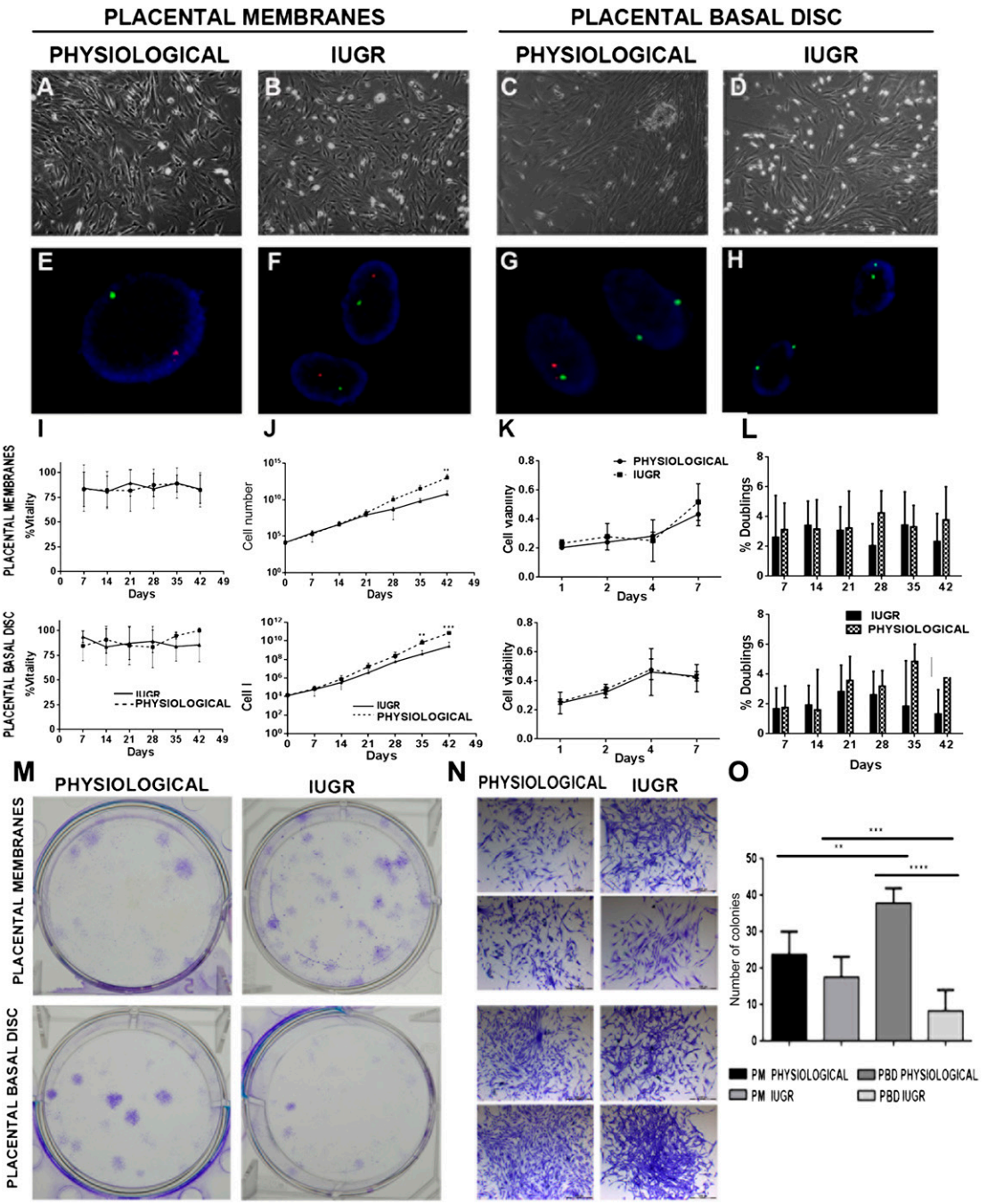

Figure 1. Characterization and proliferation of placental mesenchymal stromal cells (pMSCs). **(A–D):** Morphology of pMSCs at passage 3 isolated from the indicated placental compartment (physiological, $n = 5$; IUGR $n = 6$) observed by phase-contrast microscopy (original magnification, ×10). Fluorescent in situ hybridization analysis shows a male pattern **(E, F)**, a mixed male/female pattern **(G)**, and a female pattern **(H)**. **(I):** Viability of cells isolated from physiological ($n = 5$ each group) and IUGR ($n = 6$ each group) PM and PBD placentas after 6 weeks of culture in proliferation medium. *DXZ1* (Xp11.1q11.1) spectrum green; *SRY* (Yp11.3) spectrum orange. **(J):** Expansion rate of the same samples observed during 6 weeks of culture obtained by visual counting after trypan blue staining. Data are shown as average ± SD (in percentages) of 11 placental samples, each performed in three replicates. *, $p < .01$; ***, $p < .001$. **(K):** Proliferative potential of pMSCs isolated from physiological and IUGR PM and PBD cultured at passage (P3) was measured by 3-[31]-2,5-diphenyltetrazolium bromide assay after 0, 1, 2, 4, and 7 days of seeding. **(L):** Measurements of doubling rate every 7 days, during the entire culture period, based on visual count after trypan blue staining. **(M):** Crystal violet-stained plates of colony-forming units-fibroblast (CFU-F) assays performed on P3 pMSCs isolated from physiological and IUGR PM and PBD. **(N):** Representative phase-contrast microscopic images of single CFU-F assay of P3 pMSCs from physiological and IUGR PM and PBD stained by crystal violet (original magnification, ×4). **(O):** CFU-F assay analysis. The data represent the mean ± SEM number of colonies per plate. Abbreviations: IUGR, intrauterine growth restriction; PBD, placental basal disc; PM, placental membrane.

Published Ahead of Print on March 8, 2016 as 10.5966/sctm.2015-0155.

Morphologic and Cytogenetic Analysis of PM and PBD-Derived Cells Isolated From Physiological and IUGR Placentas

Cells were isolated from PM and PBD tissues and cultured in expansion medium. PM- and PBD-derived cells adhered to plastic and showed a typical fibroblastic morphology of MSC by light microscopy (Fig. 1A–2D).

Given the risk for cross-contamination between fetal and maternal cells, we first analyzed physiological (n = 3) and IUGR (n = 3) PM- and PBD-derived cells by fluorescence in situ hybridization (FISH) to verify that pure cell populations had been isolated. For these experiments, PM- and PBD-derived cells were isolated from placentae of women delivering a male baby, and approximately 200 cells of each type were analyzed for signals in interphase nuclei using X/Y chromosome probes. Cells derived from PM showed the XY phenotype (spectrum green and orange-labeled chromosomes, respectively) and were therefore 100% male (Fig. 1E, 1F) as previously described [34]. Two spectrum green-labeled X chromosomes were visible in cells derived from PBD with a low contamination (<5%) of XY phenotype; therefore, these cells were prevalently of maternal origin (Fig. 1G, 1H), in agreement with the literature [9, 35]. Real-time PCR with primers for the *SRY* gene confirmed these data (data not shown).

PM- and PBD-Derived Cells Isolated From Physiological and IUGR Placentas Showed Mesenchymal Features

High cell viability was reported for 6 weeks (P5) for all the analyzed samples, confirming appropriate culture conditions (Fig. 1I). Cell proliferation was also monitored by using the MTT assay. After three passages (P3), PM- and PBD-derived cells isolated from physiological and IUGR placentas showed similar rate of proliferation (Fig. 1J, 1K) and became more homogeneous following expansion with a fibroblastic morphology characteristic of MSCs (Fig. 1). Otherwise, in long-term culture conditions (for 35 days; after P5) the IUGR PM- and PBD-derived cells displayed a lower proliferation rate and doubling time compared with healthy controls (Fig. 1L). Because placenta cultured cells were morphologically indistinguishable after passaging from MSC phenotype, it was crucial to characterize these cells for the MSC surface marker expression. Flow cytometry analysis demonstrated that 24 hours after isolation, all samples presented a heterogeneous population composed of different cell types (Figs. 2, 3), whereas after 7 days of culture PM and PBD cells acquire a homogenous immunophenotype. In particular, the number of contaminating hematopoietic cells expressing the CD34 and CD45 markers progressively diminished to less than 1% after passaging (Fig. 2), with more cells positive for CD105, CD29, CD73, and CD44 mesenchymal markers (Fig. 3), indicating a progressive enrichment of pMSC.

To verify the presence of MSCs, PM- and PBD- (n = 3 per group) derived cells from IUGR and physiological placentas at P3 were assayed for their capacity to develop colony forming unit fibroblast (CFU-F) colonies (Fig. 1M–1O). Few colonies were counted in all samples with a non–statistically significant prevalence in physiological versus IUGR PM CFU-F (23.83 $\pm$ 6.24 vs. 17.58 $\pm$ 5.55; p = .07), whereas a statistically significantly increased number of colonies was found in physiological versus IUGR PBD CFU-F (37.89 $\pm$ 4.1 vs. 8.36 $\pm$ 5.75; $p < .0001$). Methylcellulose colony assays demonstrated the absence of hematopoietic colony forming unit granulocyte (CFU-G), colony forming unit-monocyte (CFU-M), and colony forming unit-granulocyte macrophage (CFU-GM) colonies after P3 (data not shown), suggesting a simultaneous loss of hematopoietic stem cell and pMSC enrichment in our culture system.

The enrichment of pMSCs occurred earlier in IUGR than in healthy samples (Fig. 3A–3F): (a) PM-derived cells from IUGR and healthy samples were CD105/CD29 (18.8% $\pm$ 1% and 10% $\pm$ 2%, respectively; $p < .05$) and CD73/CD44 (50% $\pm$ 47% and 5% $\pm$ 1% respectively, $p < .05$), and (b) PBD-derived cells from IUGR and healthy samples were CD105/CD29 (9.5% $\pm$ 1% and 1.6% $\pm$ 0.2% respectively; $p < .05$) and CD73/CD44 (4% $\pm$ 0.5% and 2% $\pm$ 0.1% respectively; $p < .05$) (Fig. 3). After 7 days of culture, the percentage of PM- and PBD-derived cells with mesenchymal immunophenotype was, respectively, 1.6–4-fold (Fig. 3C) and 2.3–5.8-fold (Fig. 3F) higher in IUGR compared with healthy controls. Differences turned out to be statistically significant for CD105, CD44, CD73, and CD90 ($p < .05$) and for CD29 ($p < .001$) expression in PM-derived cells (Fig. 3C) and only for CD29 ($p < .05$) in PBD-derived cells (Fig. 3F). After 30 days of culture, all PM- and PBD-derived cells were positive for typical MSC markers CD44, CD105, CD29, CD90, and CD73 (Fig. 3A–3F) and were negative for CD31 endothelial marker (data not shown). Overall, the data were consistent with the expression profile stipulated for pMSCs.

Multipotency of pMSCs

Differentiation of expanded pMSCs from PD and PBD of healthy and IUGR placentas into osteogenic, adipogenic, and chondrogenic lineages was examined to further verify their in vitro MSC properties. Alizarin red-stained calcium deposits indicative of bone formation were visible in pMSCs of all samples maintained in osteogenic induction medium (Fig. 4A). Oil Red O-stained lipid droplets were observed around cell nuclei in pMSCs stimulated in adipogenic differentiation medium (Fig. 4A–4C). In this condition, the IUGR pMSCs differentiated 1.7-fold more than did physiological ones, as confirmed by the number of cells expressing fatty acid binding protein 4 (FABP4) and perilipin A (data not shown). In chondrogenic conditions, the pMSCs were positive for alcian blue staining (Fig. 4A); however, no significant differences were observed between the healthy and IUGR PD and PBD groups. To determine whether IUGR affected pMSC multipotency more broadly, we evaluated the ability of pMSCs to differentiate into other cell types, specifically muscle cells. Human desmin and α-SMA-positive myotubes were formed in both IUGR and physiological groups on day 10. No significant differences were observed in the percentages of desmin-expressing cells/total nuclei when the two groups were compared (data not shown). Collectively, these in vitro findings demonstrate the multipotency of healthy and IUGR-derived pMSCs and a prevalence of adipocyte differentiation in IUGR pMSCs.

In Vitro and *In Vivo* Angiogenic Potential of pMSCs Isolated From Physiological and IUGR Placentas

Under endothelial growth medium, we observed thicker capillaries, creating a complex network predominantly in PBD-derived pMSCs (Fig. 5A). The specificity of the observed capillary structures was confirmed by their complete positivity for vWF and negativity of fibroblast cells used as negative control (Fig. 5A). Moreover, endothelial tubular structures were highly reduced in PM- and PBD-derived pMSCs from IUGR compared with healthy specimens (Fig. 5A). Indeed, the formation rate of the tubular structures during 72 hours of culture and their length (Fig. 5B) remained significantly lower in IUGR pMSCs than those in physiological ones ($p < .05$). Real-time PCR analysis confirmed

Published Ahead of Print on March 8, 2016 as 10.5966/sctm.2015-0155.

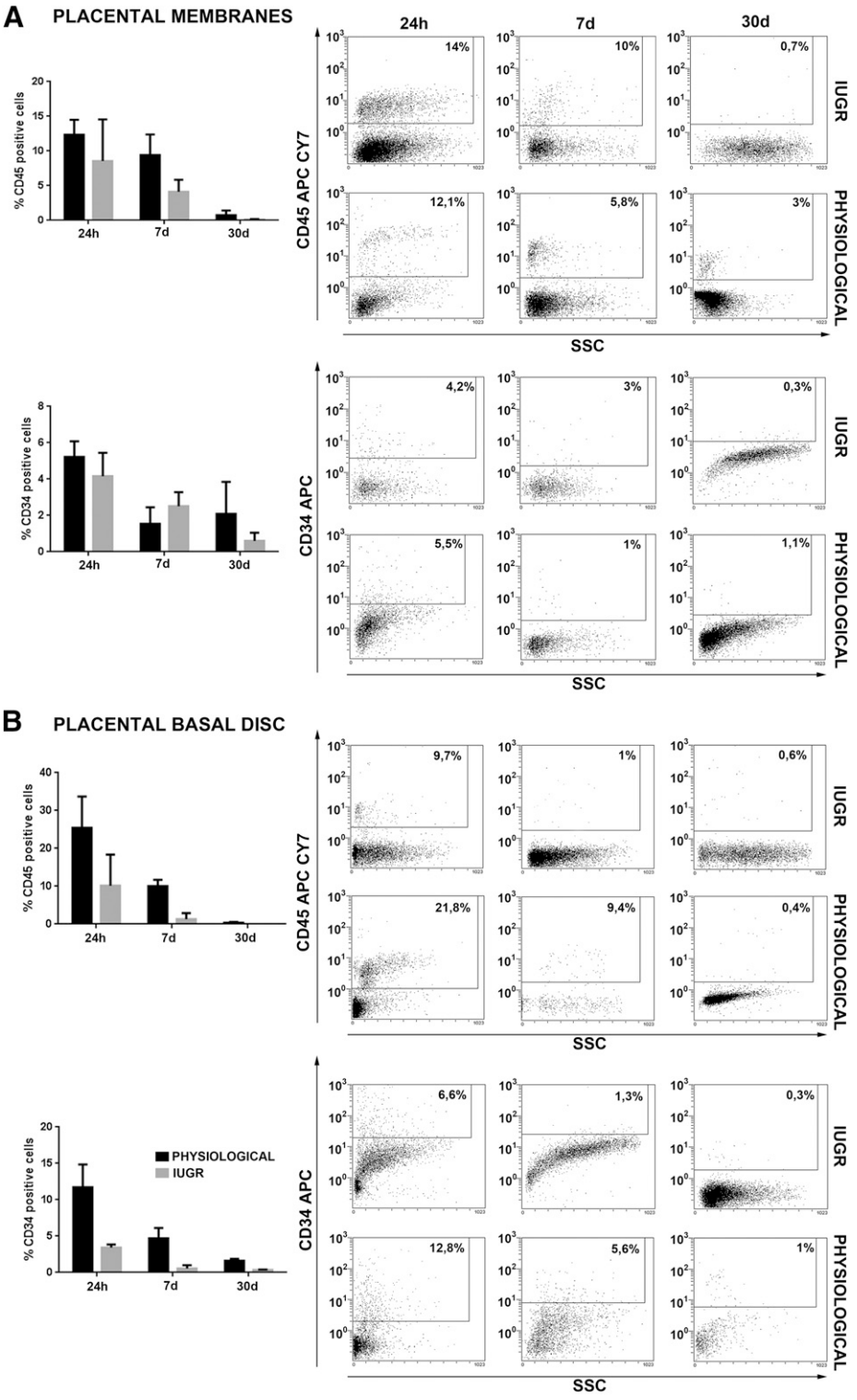

Figure 2. Flow cytometry analysis for hematopoietic antigen expression in placental mesenchymal stromal cells (pMSCs). FACScan (BD Biosciences, Franklin Lakes, NJ, http://www.bdbiosciences.com) immunophenotyping of human placental membrane- and placental basal disc (PBD)-derived cells of physiological (n = 5 each group) and IUGR (n = 6 each group) placentas. Histograms show representative examples of placental cells isolated stained with cell surface markers. Hematopoietic markers expression was analyzed 24 hours after isolation and after 7 and 30 days of culture **(A, B)**. pMSCs expressed hematopoietic markers after 24 hours of culture, which decreased considerably after 7 and 30 days of culture. The reduction of CD34 and CD45 hematopoietic markers expression was more evident in pMSC isolated from PBD-derived cells of physiological and IUGR placentas **(B)**. Abbreviations: APC, allophycocyanin; IUGR, intrauterine growth restriction; SSC, side scatter.

Published Ahead of Print on March 8, 2016 as 10.5966/sctm.2015-0155.

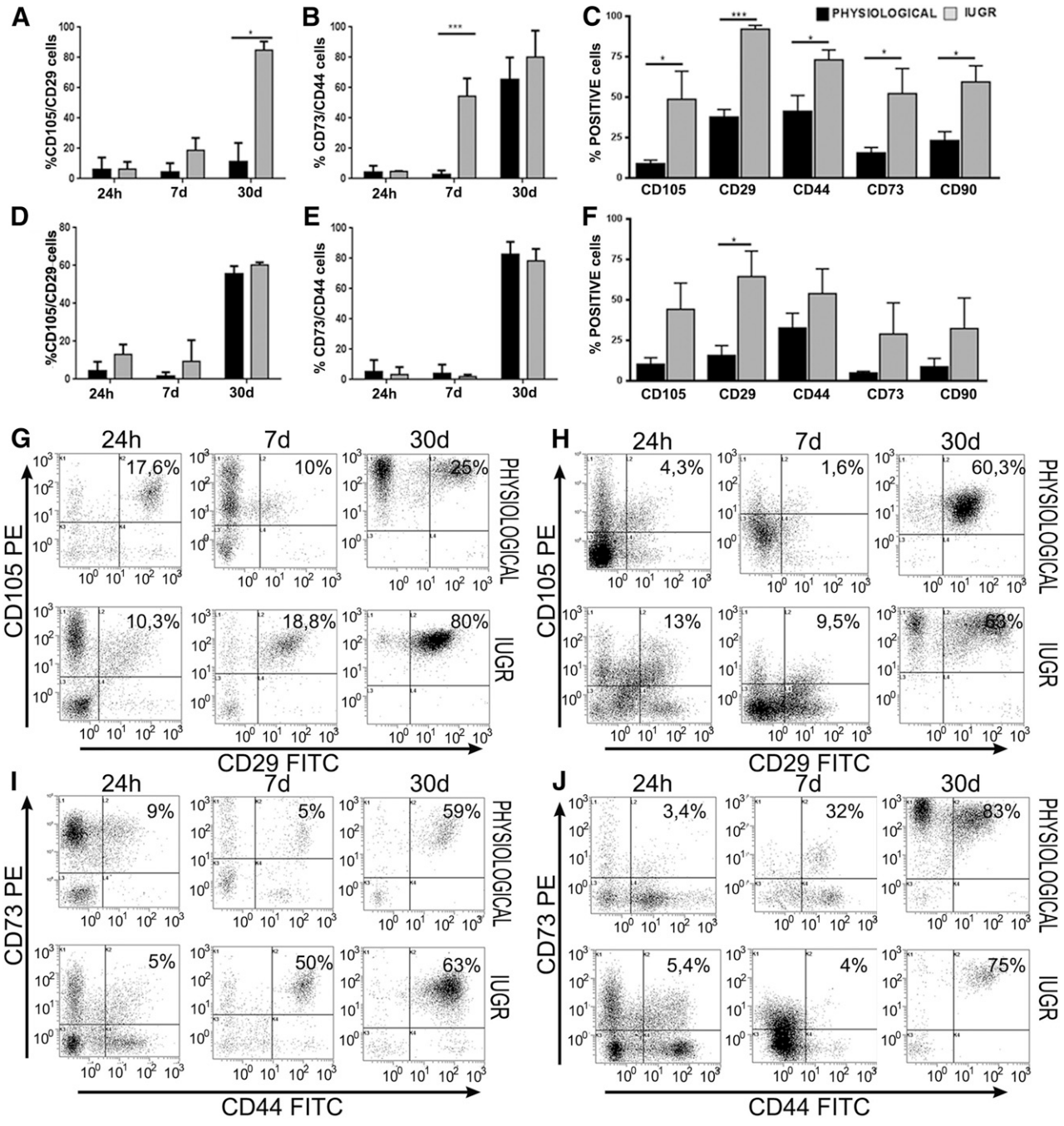

Figure 3. Flow cytometry analysis for mesenchymal antigen expression in placental mesenchymal stromal cells (pMSCs). FACScan (BD Biosciences) immunophenotyping of human placental membrane (PM)- and placental basal disc (PBD)-derived cells of physiological (n = 5 each group) and intrauterine growth restriction (IUGR) (n = 6 each group) placentas. **(A, B, D, E):** Histograms show representative examples of pMSCs isolated from passage 3 stained with mesenchymal cell surface markers. Coexpression of CD105/CD29 and CD44/CD73 increased during PM and PBD cell culture. At day 7, mesenchymal markers were 1.6–4-fold (membranes) and 2.3–5.8-fold (basal disc) higher in IUGR placentas compared with controls. Differences were statistically significant for CD105, CD44, CD73, and CD90 ($p < .05$) and for CD29 ($p < .001$) in placental membranes **(C)** and only for CD29 ($p < .05$) in placental basal disc **(F)**. *, $p < .05$; ***, $p < .001$. Moreover, dot plots show representative examples of coexpression of more significant mesenchymal markers, such as CD105+ CD29+ and CD44+CD73+ at different days of culture **(G–J)**. After 30 days, all samples showed a typical homogeneous immunophenotype of mesenchymal stromal cells. Abbreviations: FITC, fluorescein isothiocyanate; PE, preeclampsia.

statistically significantly higher CD31 expression ($p < .05$) in physiological compared with IUGR differentiated pMSCs (Fig. 5C).

The angiogenic effect of pMSC isolated from physiological and IUGR placental membranes and placental basal discs was evaluated indirectly by incubating pMSC-conditioned media with a human umbilical vein endothelial cell (HUVEC) cell line. After 24 hours, we observed a higher, non–statistically significant formation of capillary-like tube structures in PBD than PM-derived medium conditions (Fig. 5D). To further extend these in vitro data, we performed in vivo experiments using a previously described

Published Ahead of Print on March 8, 2016 as 10.5966/sctm.2015-0155.

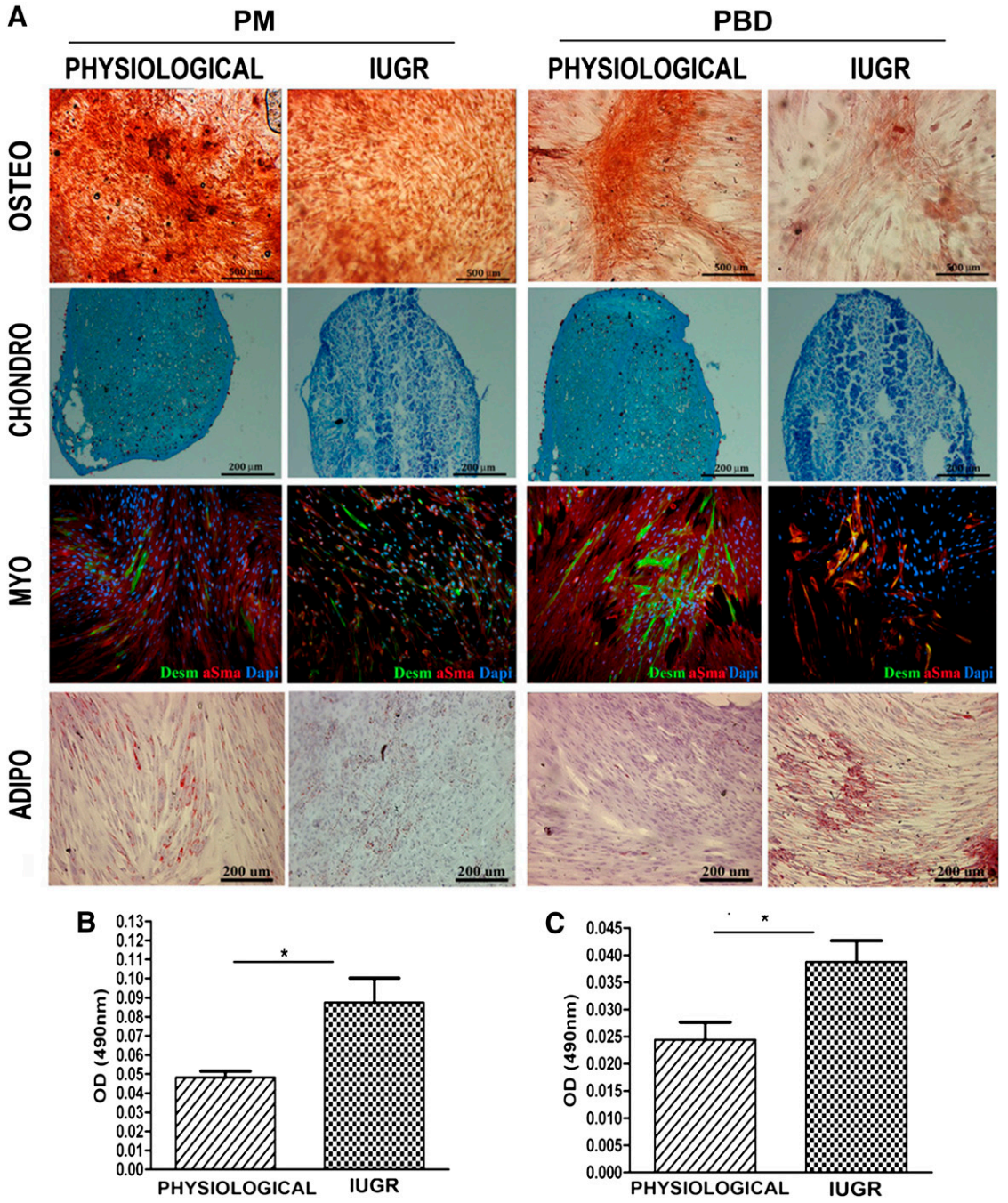

Figure 4. Placental mesenchymal stromal cell (pMSC) multilineage differentiation in vitro: osteogenic, chondrogenic, adipogenic, and myogenic commitment. pMSC isolated from placenta membrane and placental basal disc physiological (n = 5 each group) and IUGR (n = 6 each group) placentas at passage 3 were investigated for their in vitro multilineage differentiation capacity. **(A):** Osteogenesis was demonstrated by enhancement of the alizarin red staining. Chondrogenesis was indicated by alcian blue staining in cryosections from pMSCs. Desmin (green) and α-smooth muscle acti (red) staining confirmed their myogenic differentiation. Nuclei were stained blue with 4′,6-diamidino-2-phenylindole. Adipogenesis was detected by the formation of neutral lipid vacuoles stainable with Oil-Red O (for all representative examples, original magnification, $\times$10). **(B, C):** Adipogenic differentiation was quantified by spectrophotometric measurements with Oil Red O levels. $*$, $p < .05$. Abbreviations: adipo, adipogenic; chondro, chondrogenic; Dapi, 4′,6-diamidino-2-phenylindole; IUGR, intrauterine growth restriction; myo, myogenic; osteo, osteogenic.

reproducible and quantitative angiogenesis assay (DIVAA system) [32]. Fifteen days after subcutaneous implantation in nude mice, the angioreactors containing IUGR and physiological pMSCs showed numerous blood vessels positive for vWF expression (Fig. 6). A well-organized network of vessels was found in the fibroblast growth factor-2-positive control (8.8 $\pm$ 2.4) and in the samples containing pMSCs derived from PM and PBD physiological (27.4 $\pm$ 8.4 and 25.3 $\pm$ 3.2 respectively) and IUGR (10.6 $\pm$ 2.8 and 8 $\pm$ 1.6 respectively) samples (Fig. 6). Few endothelial structures were also found in the Matrigel-negative control group (5 $\pm$ 1.4) (Fig. 6). All these data suggest an impaired endothelial potential of IUGR pMSCs.

Published Ahead of Print on March 8, 2016 as 10.5966/sctm.2015-0155.

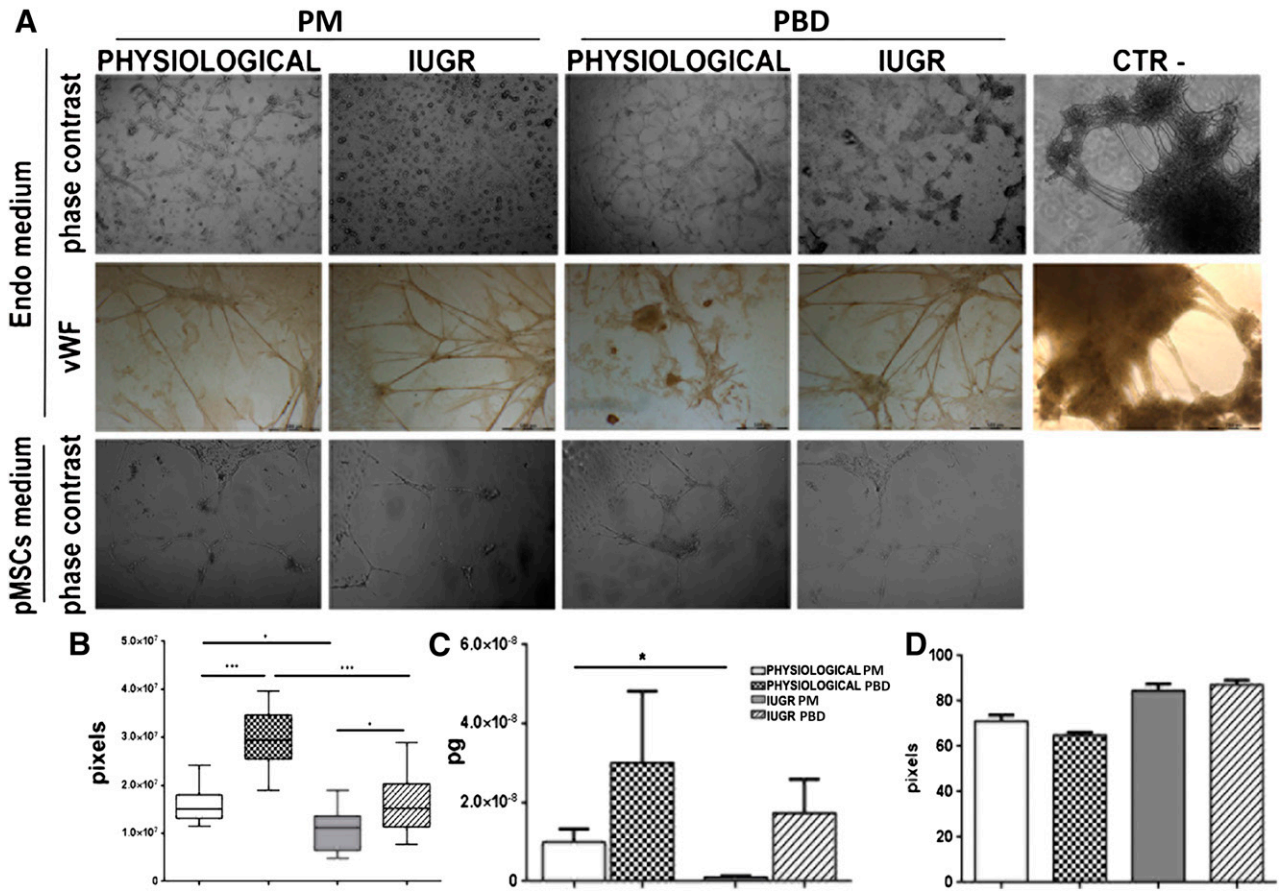

Figure 5. Tubulo formation assay. Endothelial differentiation potential of pMSCs was analyzed by immunofluorescent and immunohistochemistry assays. **(A):** Phase-contrast morphology of PM-derived pMSCs isolated from physiological ($n = 5$) and IUGR ($n = 6$) and PBD-derived pMSCs isolated from physiological ($n = 5$) and IUGR ($n = 6$) and human fibroblasts used as negative control after 72 hours of two-dimensional endothelial differentiation (original magnification, ×10). Physiological pMSCs formed more capillary-like tube structures than IUGR pMSCs. In fibroblast cells, we never observed tubular structures. These data were confirmed by quantification of endothelial differentiation, measuring tube-like structure length **(B)**, histological coloration with vWF **(A)**, and CD31 expression by real-time polymerase chain reaction analysis **(C)**. *, $p < .05$; **, $p < .005$; ***, $p < .001$. The angiogenic effect of pMSCs was indirectly measured by incubating pMSC-conditioned medium with human umbilical vein endothelial cell line in a Matrigel tube formation assay **(A)** and quantified by measuring tube-like structure length **(D)**. Abbreviations: IUGR, intrauterine growth restriction; CTR-, negative control; Endo medium, two-dimensional endothelial differentiation; PD, placental basal disc; PM, placental membrane; pMSCs medium, placental mesenchymal stromal cell-conditioned medium; vWF, von Willebrand factor.

Activation of Respiratory Mitochondria-Related Genes in IUGR pMSCs

Because we observed a reduced endothelial potential in IUGR pMSCs, we hypothesized that environmental placental hypoxia may influence the respiratory mitochondria gene expression of these cells. Indeed, recent literature demonstrated that mitochondrial dysfunction also represents a critical factor for fetal programming in cases of placental insufficiency [36]. We therefore investigated the expression levels of the respiratory chain genes *UQCRC1* and *COX4I1* and of the mitochondrial biogenesis activator *NRF1* in IUGR ($n = 3$) and physiological ($n = 3$) pMSCs. IUGR compared with physiological pMSCs displayed a trend toward higher levels of all analyzed genes in the PBD and of *COX4I1* in PM groups ($p < .05$) (Fig. 7). These data may suggest a role of the pMSCs in IUGR and are in agreement with our previously reported results [18].

Discussion

Here we report for the first time pMSC proliferation and differentiation characteristics in human IUGR pregnancies. Mesenchymal marker enrichment and multipotent differentiation abilities confirmed successful isolation and selection of a mesenchymal stromal cell population from membranes and basal disc of both physiological and IUGR placentas. As attested by flow cytometry data, the pMSC population was selected earlier in IUGR placentas, although initial cell type proportions were similar in the two groups. Moreover, this population displayed lower endothelial and higher adipogenic differentiation potentials compared with normal controls. We found lower proliferation rate in IUGR pMSCs compared with controls, especially after 35 days of culture.

A significant decrease in pMSC proliferation rate has been previously reported in PE with fetal and/or placental compromise compared with physiological pregnancies [24]. Authors hypothesized that this pMSC reduction could impair primary villi formation and trophoblast development during placentation because pMSCs both serve as structural support and exert a paracrine activity on trophoblast cells. Thus, this could contribute to the abnormal villous architecture found in PE [1, 24]. Decreased proliferation was also found in MSCs isolated from PE deciduas, and linked to microRNA-16 (miR-16) overexpression leading to

Published Ahead of Print on March 8, 2016 as 10.5966/sctm.2015-0155.

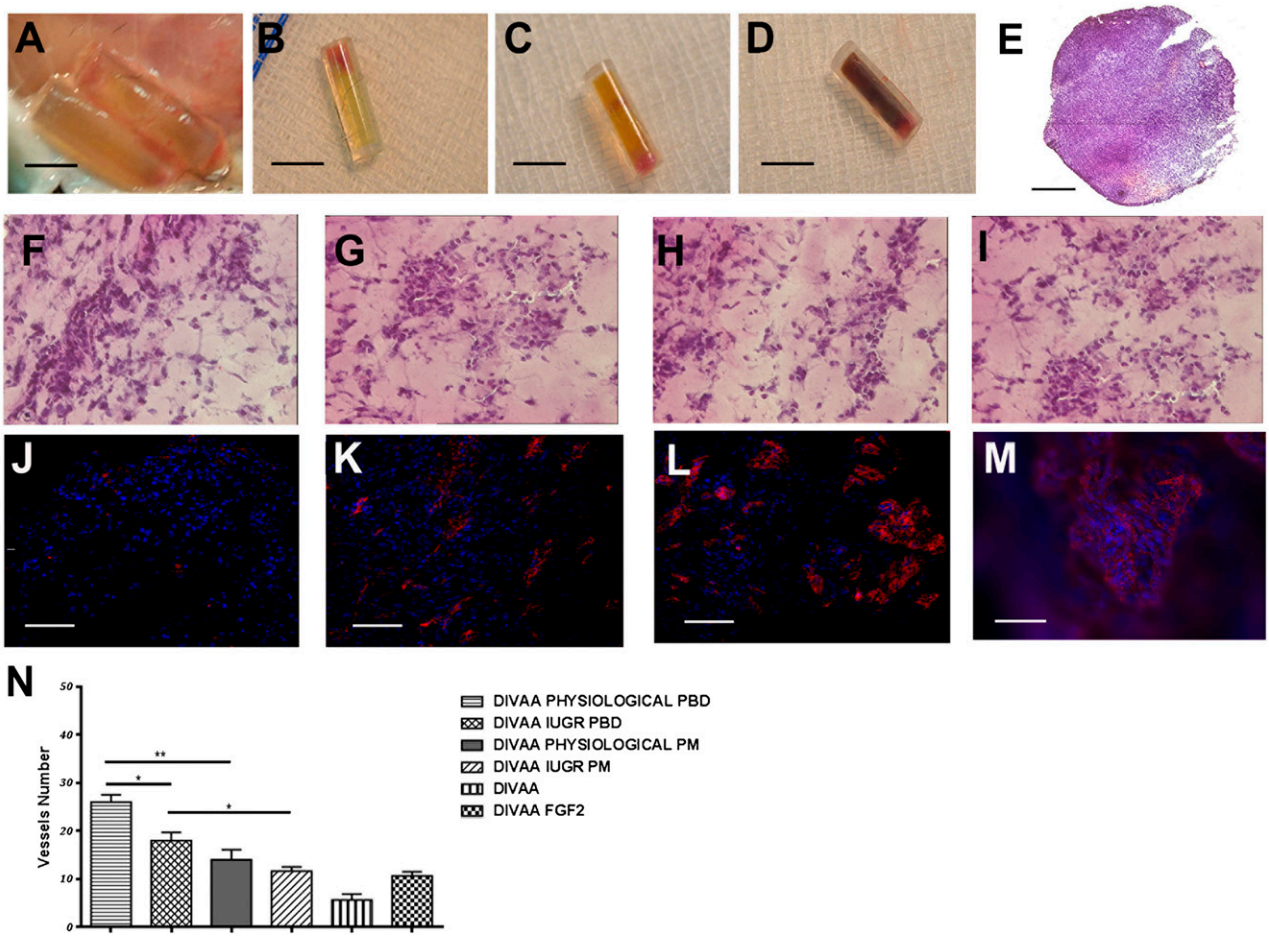

Figure 6. Angiogenic potential of placental mesenchymal stromal cells (pMSCs) isolated from human physiological and intrauterine growth restriction (IUGR) placentas. Quantification of angiogenic activity of PM- and PBD-derived pMSCs isolated from physiological and IUGR performed by the DIVAA system. **(A):** Angioreactors were recovered at 15 days after subcutaneous implantation. Unlike the control angioreactors with no angiogenic factor **(B)**, assays containing an angiogenic factor (fibroblast growth factor-2 [FGF-2]) **(C)** and human pMSCs only **(D)** revealed numerous blood vessels near the open end that invade the Matrigel. Sections of paraffin-embedded angioreactor containing pMSCs stained by hematoxylin and eosin (H&E) **(E)** (original magnification, ×10), and H&E staining of angioreactor containing physiological and IUGR PBD-derived pMSCs **(F, G)** and physiological and IUGR PM-derived pMSCs **(H, I)** (original magnification, ×40). Matrigel invasion and early organization of endothelial cell-containing structures is revealed by vWF (in red) (angioreactor only **[J]**, angioreactor plus FGF-2 **[K]**, and the angioreactor with physiological and IUGR PBD-derived pMSCs **[L, M]**). PBD-derived pMSCs isolated from physiological and IUGR spread throughout the surface and aligned to form branching, anatomizing tubes with multicentric junctions that formed a closely knit meshwork of capillary-like structures **(L, M)**. The number of von Willebrand factor-positive vessels represented in **(N)** was obtained by counting six fields at original magnification, ×20 (*, $p < .05$; **, $p < .005$). Abbreviations: DIVAA, directed in vivo angiogenesis angioreactor; PD, placental basal disc; PM, placental membrane.

cyclin E1 downregulation. High miR-16 levels also caused VEGF subtype A and decreased secretion and led to consequent reduction of trophoblast migration, HUVEC migration, and blood vessel formation. It was therefore suggested that abnormal decidual MSCs overexpressing miR-16 may be involved in PE development by altering the pregnancy microenvironment that influences angiogenic processes [25].

As attested by flow cytometry, in IUGR placentas the mesenchymal stromal cell population is selected earlier than seen with controls. This suggests that in the pathological tissue-specific conditions might occur so that mesenchymal stromal cells are more resistant and selected faster. However, IUGR pMSCs showed a low rate of proliferation and altered differentiation capacities toward endothelial and adipogenic lineages. Thus, the faster selection of the mesenchymal cell type in IUGR cultures might represent a compensatory mechanism to metabolic alterations occurring in IUGR placental cells and/or to the adverse IUGR placental environment.

Our data showed lower endothelial differentiation potential of pMSCs isolated from IUGR placentas compared with healthy controls. Placental mesenchymal cells have been proposed to play an important role in placental vascularization during the whole human pregnancy by contributing both to vasculogenesis and angiogenesis, which are critical for placental development [20]. Abnormal vasculogenesis and angiogenesis are correlated with the impaired placental and fetal development observed in complicated pregnancies, such as IUGR [20]. Interestingly, in vitro studies showed that IUGR placental villous stromal cells altered ability to stimulate endothelial tubule-like structure formation and migration [37]. In addition, the imbalance between pro- and antiangiogenic factors is well documented in placentas and in maternal blood of IUGR and PE pregnancies, suggesting a role in their pathophysiology [38, 39]. Endothelial progenitors contribute to tissue regeneration by induction of new vessels, thereby increasing tissue perfusion and oxygenation [40, 41]. The

Published Ahead of Print on March 8, 2016 as 10.5966/sctm.2015-0155.

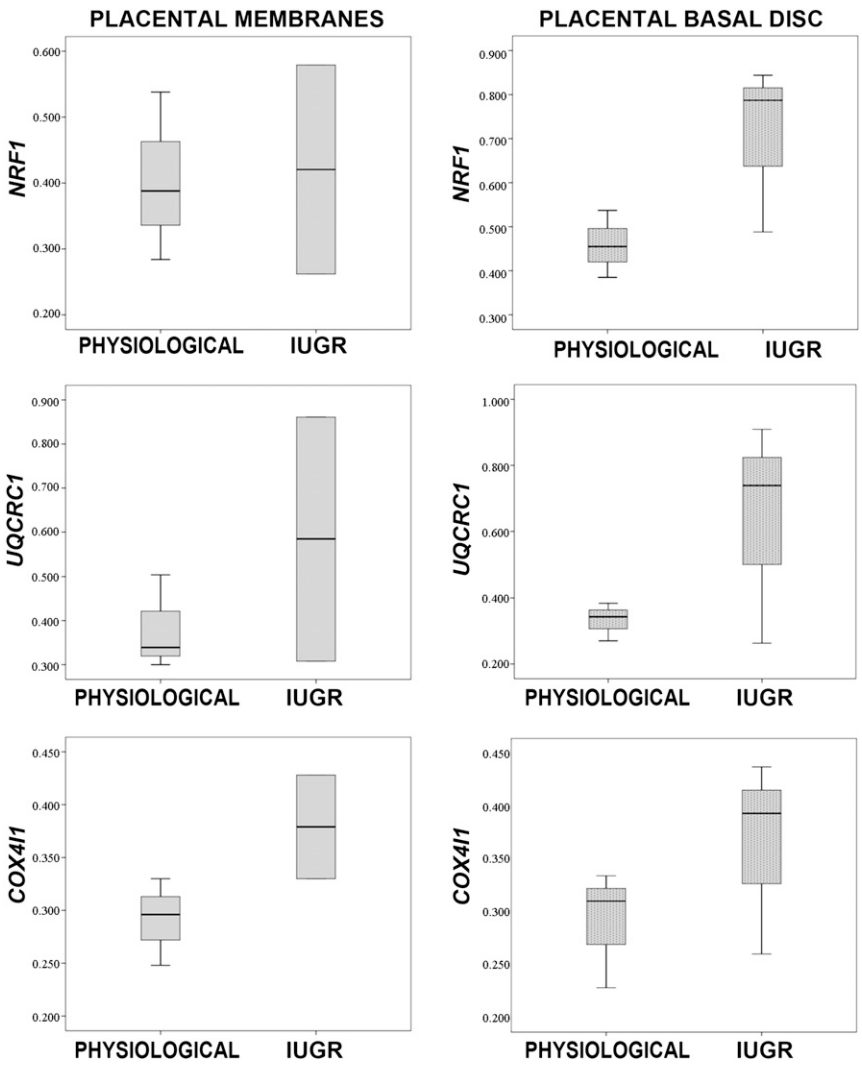

Figure 7. Gene expression analysis of mitochondrial biogenesis activator and respiratory chain complexes of placental mesenchymal stromal cells (pMSCs). Gene expression of *NRF1* (mitochondrial biogenesis activator), *UQCRC1*, and *COX4I1* (mitochondrial respiratory chain subunits) in placental membrane- and placental basal disk-derived pMSCs isolated from five physiological and six IUGR pregnancies. Relative expression values are shown as box plots, indicating the median and the 25th and 75th percentiles. Abbreviation: IUGR, intrauterine growth restriction.

formation of these networks is important for organogenesis during fetal development. Indeed, endothelial progenitor cells play a critical role in blood vessel formation and vascular homeostasis and can also lead to tissue disorganization and fibrosis, as reviewed by Piera-Velazquez et al. [42].

Interestingly, several studies have pinpointed alterations in maternal and fetal endothelial progenitor cells [43, 44]. The mechanisms underlying impaired neovascularization in feto-placental circulation occurring in IUGR still need to be clarified and may be associated with the reduced capacity of pMSCs to give rise to differentiated endothelial cells. Unlike endothelial differentiation capacity, we found increased adipogenic potential in IUGR pMSCs compared with controls. To our knowledge, pMSC adipogenic potential has never been quantitatively assessed in the pathologic human placenta. However, IUGR newborns have increased risk for adult obesity and metabolic syndrome [45].

In animal models of IUGR, several alterations involving both the adipose tissue structure and endocrine system have been demonstrated. Changes in central nervous system appetite control and hormone secretion and regulation, as well as an increase of adipocyte differentiation, have been shown in IUGR rat offspring, as reviewed by Desai and Ross [45]. Because these changes are evident early in life, the predisposition to obesity may be programmed in utero, as already hypothesized in the "fetal programming" theory [46], possibly through altered epigenetic mechanisms as recently reported in rat offspring [47]. Mitochondrial dysfunctions also represent a critical factor for fetal programming in cases of placental insufficiency [36]. Diaz and colleagues showed the link between fetal growth restraint and placental mitochondrial dysfunction, as reflected by changes in mitochondrial DNA (mtDNA) content and superoxide dismutase activity [48].

Because we previously demonstrated that mtDNA content was high in IUGR placentas [18], we investigated the gene expression levels of the mitochondrial respiratory chain genes *UQCRC1* and *COX4I1* (respectively belonging to the III and IV respiratory chain complex) and of the mitochondrial biogenesis activator *NRF1* of IUGR and healthy pMSCs. Mesenchymal stem cell metabolism is known to be mainly anaerobic. The shift toward an aerobic mitochondrial metabolism is reported during differentiation, with increase of mitochondrial biogenesis, oxygen consumption, and

Published Ahead of Print on March 8, 2016 as 10.5966/sctm.2015-0155.

ATP production [49]. Thus, mitochondrial modifications might account for the higher adipogenic and the lower endothelial differentiation ability of pMSCs derived from IUGR placentas. Interestingly, pMSCs cultured with no differentiating medium presented a trend toward higher *NRF1*, *UQCRC1*, and *COX4I1* expression levels in IUGR basal disc samples compared with controls and higher *COX4I1* levels in IUGR placental membranes. These differences were not statistically significant, probably because of the low sample number. Nevertheless, they might account for metabolic alterations in IUGR pMSCs, showing a possible shift to aerobic metabolism, with the loss of the metabolic characteristics that are typical of multipotent and undifferentiated cells. This might be due to differences in oxygen concentrations within the placenta, occurring in IUGR [50, 51], regulating mitochondrial biogenesis and function, as previously observed in other animal tissues [52, 53].

We recently showed higher mitochondrial content in IUGR placental tissue; this content was decreased in cytotrophoblast cells isolated from the same placentas [18, 19]. We hypothesized that other cell types may be responsible for the mitochondrial content increase in the entire placental tissue, despite the decrease in cytotrophoblast cells. Here we suggest that pMSCs might contribute to the global mitochondrial content increase in IUGR compared with control placental tissues, possibly together with other placental cells, such as endothelial cells.

A potential limitation of this study is represented by the different gestational age of the IUGR compared with the control group. This is a limit of all studies comparing human IUGR to control term placentas because IUGR pregnancies are electively delivered earlier in the interest of the fetus. Another potential limitation is that we investigated IUGR placentas at delivery, whereas placental abnormal development is supposed to start at the beginning of placentation. Therefore, a cause-effect relationship may not be inferred because the observed features might also be the consequence of the altered placental environment influencing pMSCs. In the developing embryo, subtle changes in the microenvironment drive epigenetic change associated with cellular differentiation [54]. However, this inherent sensitivity to external influence, which is a hallmark of early development, potentially renders epigenetic marks of pMSCs susceptible to external environmental influence. At present, no strong evidence exists for a role of epigenetic disruption as a driver of IUGR [55].

Interestingly, we demonstrated a fetal origin of the PM-derived pMSCs and a maternal low contamination of PBD pMSCs. These data agree with the literature [34, 56] and pointed out whether maternal pMSCs may be involved in IUGR disease. Thus, further studies are required to better understand the role of pMSCs in IUGR and how environmental influence on placental functioning modulate their regenerative capacities.

Conclusion

The observed IUGR-specific features may indicate a role of pMSCs in determining the specific placental phenotype associated with IUGR pathogenesis. The loss of endothelial differentiation potential and the increase of adipogenic ability that we report are likely to contribute to the vicious cycle of abnormal placental development in IUGR. These genuine new findings fit well with what is already known about placental pathological features in IUGR. Targeting pMSCs may thus lead to new perspectives for the treatment of IUGR.

Acknowledgments

We thank all the midwives and nurses of the Unit of Obstetrics and Gynecology of the L. Sacco Hospital in Milan for their competence and cooperation. We also thank all the pregnant patients for participating in the study. This work was financially supported by grants from Fondazione Giorgio Pardi and from the Italian Ministry of University and Research PRIN 2010-2011 prot. 20102chst5_005 "Parto pre-termine: markers molecolari, biochimici e biofisici dell'unità feto-placentare" (to I.C.). It was also supported by Associazione Amici del Centro Dino Ferrari, Associazione Amici di Emanuele, and Fondazione Opsis Onlus (to Y.T.).

Author Contributions

C.M.: conception/design, provision of study materials or patients, manuscript writing; P.R.: collection and/or assembly of data, data analysis and interpretation; C.N.: collection and/or assembly of data; G.M.A., SE., S.B., M.M., A.T., M.B., A.R., and S.M.: performance of experiments; M.B.: data analysis and interpretation, manuscript writing; Y.T.: conception/design, data analysis and interpretation, manuscript writing, final approval of manuscript; I.C.: conception/design, provision of study materials or patients, data analysis and interpretation, manuscript writing, final approval of manuscript.

Disclosure of Potential Conflicts of Interest

The authors indicated no potential conflicts of interest.

References

1 Nuzzo AM, Giuffrida D, Zenerino C et al. JunB/cyclin-D1 imbalance in placental mesenchymal stromal cells derived from preeclamptic pregnancies with fetal-placental compromise. Placenta 2014;35:483–490.

2 Dominici M, Le Blanc K, Mueller I et al. Minimal criteria for defining multipotent mesenchymal stromal cells. The International Society for Cellular Therapy position statement. Cytotherapy 2006;8:315–317.

3 Brooke G, Tong H, Levesque JP et al. Molecular trafficking mechanisms of multipotent mesenchymal stem cells derived from human bone marrow and placenta. Stem Cells Dev 2008;17:929–940.

4 Yen BL, Huang HI, Chien CC et al. Isolation of multipotent cells from human term placenta. Stem Cells 2005;23:3–9.

5 Abumaree MH, Al Jumah MA, Kalionis B et al. Phenotypic and functional characterization of mesenchymal stem cells from chorionic villi of human term placenta. Stem Cell Rev 2013;9:16–31.

6 Castrechini NM, Murthi P, Gude NM et al. Mesenchymal stem cells in human placental chorionic villi reside in a vascular Niche. Placenta 2010; 31:203–212.

7 In 't Anker PS, Scherjon SA, Kleijburg-van der Keur C et al. Isolation of mesenchymal stem cells of fetal or maternal origin from human placenta. Stem Cells 2004;22:1338–1345.

8 Witkowska-Zimny M, Wrobel E. Perinatal sources of mesenchymal stem cells: Wharton's jelly, amnion and chorion. Cell Mol Biol Lett 2011;16:493–514.

9 Heazlewood CF, Sherrell H, Ryan J et al. High incidence of contaminating maternal cell overgrowth in human placental mesenchymal stem/stromal cell cultures: a systematic review. Stem Cells Translational Medicine 2014;3: 1305–1311.

10 James JL, Srinivasan S, Alexander M et al. Can we fix it? Evaluating the potential of placental stem cells for the treatment of pregnancy disorders. Placenta 2014;35:77–84.

11 Make Every Mother and Child Count. Geneva, Switzerland: World Health Organization, 2005.

12 ACOG Committee on Practice Bulletins–Obstetrics. ACOG practice bulletin. Diagnosis and management of preeclampsia and eclampsia. Number 33, January 2002. Obstet Gynecol 2002;99:159–167.

13 Cetin I, Alvino G.. Intrauterine growth restriction: Implications for placental metabolism and transport. A review. Placenta 2009;30: (suppl A):S77–S82.

Published Ahead of Print on March 8, 2016 as 10.5966/sctm.2015-0155.

14 Cetin I, Mandò C, Calabrese S. Maternal predictors of intrauterine growth restriction. Curr Opin Clin Nutr Metab Care 2013;16:310–319.

15 Mandò C, Tabano S, Colapietro P et al. Transferrin receptor gene and protein expression and localization in human IUGR and normal term placentas. Placenta 2011;32:44–50.

16 Mandò C, Tabano S, Pileri P et al. SNAT2 expression and regulation in human growth-restricted placentas. Pediatr Res 2013;74:104–110.

17 Pardi G, Cetin I, Marconi AM et al. Diagnostic value of blood sampling in fetuses with growth retardation. N Engl J Med 1993;328:692–696.

18 Lattuada D, Colleoni F, Martinelli A et al. Higher mitochondrial DNA content in human IUGR placenta. Placenta 2008;29:1029–1033.

19 Mandò C, De Palma C, Stampalija T et al. Placental mitochondrial content and function in intrauterine growth restriction and preeclampsia. Am J Physiol Endocrinol Metab 2014;306:E404–E413.

20 Gourvas V, Dalpa E, Konstantinidou A et al. Angiogenic factors in placentas from pregnancies complicated by fetal growth restriction (review). Mol Med Rep 2012;6:23–27.

21 Chen CP, Huang JP, Chu TY et al. Human placental multipotent mesenchymal stromal cells modulate trophoblast migration via Rap1 activation. Placenta 2013;34:913–923.

22 Hwang JH, Lee MJ, Seok OS et al. Cytokine expression in placenta-derived mesenchymal stem cells in patients with pre-eclampsia and normal pregnancies. Cytokine 2010;49:95–101.

23 Portmann-Lanz CB, Baumann MU, Mueller M et al. Neurogenic characteristics of placental stem cells in preeclampsia. Am J Obstet Gynecol 2010;203:399, e391–397.

24 Rolfo A, Giuffrida D, Nuzzo AM et al. Pro-inflammatory profile of preeclamptic placental mesenchymal stromal cells: new insights into the etiopathogenesis of preeclampsia. PLoS One 2013;8:e59403.

25 Wang Y, Fan H, Zhao G et al. miR-16 inhibits the proliferation and angiogenesis-regulating potential of mesenchymal stem cells in severe pre-eclampsia. FEBS J 2012;279:4510–4524.

26 Figueras F, Gardosi J. Intrauterine growth restriction: New concepts in antenatal surveillance, diagnosis, and management. Am J Obstet Gynecol 2011;204:288–300.

27 Zhang J, Merialdi M, Platt LD et al. Defining normal and abnormal fetal growth: Promises and challenges. Am J Obstet Gynecol 2010;202:522–528.

28 Todros T, Ferrazzi E, Groli C et al. Fitting growth curves to head and abdomen measurements of the fetus: A multicentric study. J Clin Ultrasound 1987;15:95–105.

29 Parazzini F, Cortinovis I, Bortolus R et al. Weight at birth by gestational age in Italy. Hum Reprod 1995;10:1862–1863.

30 Jaramillo-Ferrada PA, Wolvetang EJ, Cooper-White JJ. Differential mesengenic potential and expression of stem cell-fate modulators in mesenchymal stromal cells from human-term placenta and bone marrow. J Cell Physiol 2012;227:3234–3242.

31 Berridge MV, Tan AS. Characterization of the cellular reduction of 3-(4,5-dimethylthiazol-2-yl)-2,5-diphenyltetrazolium bromide (MTT): Subcellular localization, substrate dependence, and involvement of mitochondrial electron transport in MTT reduction. Arch Biochem Biophys 1993;303:474–482.

32 Guedez L, Rivera AM, Salloum R et al. Quantitative assessment of angiogenic responses by the directed in vivo angiogenesis assay. Am J Pathol 2003;162:1431–1439.

33 Vandesompele J, De Preter K, Pattyn F et al. Accurate normalization of real-time quantitative RT-PCR data by geometric averaging of multiple internal control genes. Genome Biol 2002;3:RESEARCH0034.

34 Wang L, Yang Y, Zhu Y et al. Characterization of placenta-derived mesenchymal stem cells cultured in autologous human cord blood serum. Mol Med Rep 2012;6:760–766.

35 Semenov OV, Koestenbauer S, Riegel M et al. Multipotent mesenchymal stem cells from human placenta: cCritical parameters for isolation and maintenance of stemness after isolation. Am J Obstet Gynecol 2010;202:e191–e193.

36 Leduc L, Levy E, Bouity-Voubou M et al. Fetal programming of atherosclerosis: Possible role of the mitochondria. Eur J Obstet Gynecol Reprod Biol 2010;149:127–130.

37 Riddell MR, Winkler-Lowen B, Jiang Y et al. Fibrocyte-like cells from intrauterine growth restriction placentas have a reduced ability to stimulate angiogenesis. Am J Pathol 2013;183:1025–1033.

38 Barut F, Barut A, Gun BD et al. Intrauterine growth restriction and placental angiogenesis. Diagn Pathol 2010;5:24.

39 Levine RJ, Maynard SE, Qian C et al. Circulating angiogenic factors and the risk of preeclampsia. N Engl J Med 2004;350:672–683.

40 Charnock-Jones DS, Kaufmann P, Mayhew TM. Aspects of human fetoplacental vasculogenesis and angiogenesis. I. Molecular regulation. Placenta 2004;25:103–113.

41 Demir R, Seval Y, Huppertz B. Vasculogenesis and angiogenesis in the early human placenta. Acta Histochem 2007;109:257–265.

42 Piera-Velazquez S, Li Z, Jimenez SA. Role of endothelial-mesenchymal transition (EndoMT) in the pathogenesis of fibrotic disorders. Am J Pathol 2011;179:1074–1080.

43 Calcaterra F, Taddeo A, Colombo E et al. Reduction of maternal circulating endothelial progenitor cells in human pregnancies with intrauterine growth restriction. Placenta 2014;35:431–436.

44 Sipos PI, Bourque SL, Hubel CA et al. Endothelial colony-forming cells derived from pregnancies complicated by intrauterine growth restriction are fewer and have reduced vasculogenic capacity. J Clin Endocrinol Metab 2013;98:4953–4960.

45 Desai M, Ross MG. Fetal programming of adipose tissue: Effects of intrauterine growth restriction and maternal obesity/high-fat diet. Semin Reprod Med 2011;29:237–245.

46 Barker DJ, Eriksson JG, Forsén T et al. Fetal origins of adult disease: Strength of effects and biological basis. Int J Epidemiol 2002;31:1235–1239.

47 Desai MJ, Jellyman JK, Han G et al. Epigenetic histone modifications in adipocytes of intrauterine growth-restricted newborns: mechanism for early induction of adipocyte differentiation and programmed obesity. Reprod Sci 2014;21(suppl):82A.

48 Díaz M, Aragonés G, Sánchez-Infantes D et al. Mitochondrial DNA in placenta: Associations with fetal growth and superoxide dismutase activity. Horm Res Paediatr 2014;82:303–309.

49 Chen CT, Shih YR, Kuo TK et al. Coordinated changes of mitochondrial biogenesis and antioxidant enzymes during osteogenic differentiation of human mesenchymal stem cells. STEM CELLS 2008;26:960–968.

50 Pardi G, Cetin I, Marconi AM et al. Venous drainage of the human uterus: Respiratory gas studies in normal and fetal growth-retarded pregnancies. Am J Obstet Gynecol 1992;166:699–706.

51 Regnault TR, de Vrijer B, Galan HL et al. Development and mechanisms of fetal hypoxia in severe fetal growth restriction. Placenta 2007;28:714–723.

52 Gutsaeva DR, Carraway MS, Suliman HB et al. Transient hypoxia stimulates mitochondrial biogenesis in brain subcortex by a neuronal nitric oxide synthase-dependent mechanism. J Neurosci 2008;28:2015–2024.

53 Zungu M, Alcolea MP, García-Palmer FJ et al. Genomic modulation of mitochondrial respiratory genes in the hypertrophied heart reflects adaptive changes in mitochondrial and contractile function. Am J Physiol Heart Circ Physiol 2007;293:H2819–H2825.

54 Novakovic B, Saffery R. The importance of the intrauterine environment in shaping the human neonatal epigenome. Epigenomics 2013;5:1–4.

55 Villar J, Carroli G, Wojdyla D et al. Preeclampsia, gestational hypertension and intrauterine growth restriction, related or independent conditions? Am J Obstet Gynecol 2006;194:921–931.

56 Fukuchi Y, Nakajima H, Sugiyama D et al. Human placenta-derived cells have mesenchymal stem/progenitor cell potential. STEM CELLS 2004;22:649–658.

See www.StemCellsTM.com for supporting information available online.

